

1 **Field Testing Two Flux Footprint Models**

2 Trevor W. Coates<sup>1</sup>, Monzurul Alam<sup>2</sup>, Thomas K. Flesch<sup>3</sup>, Guillermo Hernandez-Ramirez<sup>2</sup>

3 <sup>1</sup> Agriculture and Agri-Food Canada, Lethbridge, Canada, T1J 4B1

4 <sup>2</sup> Department of Renewable Resources, University of Alberta, Edmonton, Canada T6G 2E3

5 <sup>3</sup> Department of Earth and Atmospheric Sciences, University of Alberta, Edmonton, Canada T6G 2E3

6 *Correspondence to:* Thomas Flesch ([thomas.flesch@ualberta.ca](mailto:thomas.flesch@ualberta.ca))

7 **Abstract**

8 A field study was undertaken to investigate the accuracy of two micrometeorological flux footprint models for calculating the gas  
9 emission rate from a synthetic 10 x 10 m surface area source, based on the vertical flux of gas measured at fetches of 15 to 50 m  
10 downwind of the source. Calculations were made with an easy to use tool based on the Kormann-Meixner analytical model and  
11 with a more sophisticated Lagrangian stochastic dispersion model. A total of 59 testable 10 minute observation periods were  
12 measured over nine days. On average, both models underestimated the actual release rate by approximately 30%, mostly due to  
13 large underestimates at the larger fetches. The accuracy of the model calculations had large period-to-period variability, and no  
14 statistical differences were observed between the two models in terms of overall accuracy.

15 **1 Introduction**

16 Micrometeorological techniques such as eddy covariance and flux-gradient measure a vertical flux of gas in the atmosphere, which  
17 can be used to deduce the flux from an underlying surface area of interest. If the underlying surface is expansive and horizontally  
18 homogenous, the measured atmospheric flux and the surface flux can be considered equivalent (Dyer, 1963). However, if the area  
19 of interest has a limited spatial extent, or is located some distance from the atmospheric measurement, the relationship between the  
20 two fluxes can be complex, as the measured flux may be capturing a dynamic mixture of surface fluxes from both inside and  
21 outside the area of interest. In these cases, flux footprint modelling can be used to quantify the relationship between the measured  
22 atmospheric flux and the surface flux from the area of interest.

23 The analytical flux footprint model of Kormann and Meixner (2001), hereafter referred to as the KM model, is widely used to  
24 evaluate and interpret flux measurements taken over spatially limited surface sources. The KM model relies on a simplified  
25 representation of atmospheric transport (Schmid, 2002) to create an easily computable footprint. It has been used to help quantify  
26 ammonia fluxes from fertilized plots (Spirig et al., 2010), interpret methane fluxes from heterogeneous peatland areas (Budishchev  
27 et al., 2014), and to reject periods where the footprint extends outside the source of interest (Stevens et al., 2012). Other footprint  
28 models use a more realistic treatment of atmospheric transport (e.g., Kljun et al., 2002; Sogachev and Lloyd, 2004). Using a state  
29 of the art Lagrangian stochastic (LS) footprint model, Wilson (2015) found a clear separation between the footprints computed  
30 with the LS and KM models, depending on atmospheric stability and the distance from the measurement location. While more  
31 rigorous footprint models are clearly more defensible, the simpler KM model has the advantage of rapid analysis and the existence  
32 of software tools that make its application more accessible to non-specialists (Nefel et al., 2008).

33 This field study compares the accuracy of the KM footprint model with a more rigorous LS model. The motivation for this study  
34 was the question of whether the accuracy of the LS model was sufficiently better than the KM model so as to justify a more  
35 complex LS application. In this experiment we released gas at a known rate from a small synthetic area source and measured the  
36 vertical gas flux at a downwind location using the eddy covariance technique. The KM and LS models were then used to calculate  
37 the source emission rate from the measured atmospheric flux. The accuracy of those calculations is examined in this report. This  
38 follows the approach of Heidbach et al. (2017) and Coates et al. (2017) in their experimental evaluation of footprint models.

## 39 2 Methods

### 40 2.1 Gas Release

41 The experiment took place on an extensive, flat agricultural field at the University of Alberta's Breton Research Farm, in Alberta,  
42 Canada (53° 07' N, 114° 28' W). Measurements were made after autumn harvest, and the surface was rye (*Secale cereale* L.)  
43 stubble with an average height of 3 cm. No obstructions to the wind were present within 250 m of the measurement site.

44 A synthetic source of carbon dioxide (CO<sub>2</sub>) gas was constructed using 10 lengths of ½" (12.7 mm) diameter PVC pipe, each 10 m  
45 long. The 10 pipes were loosely positioned to create a nominal 10 x 10 m square source area. Compressed CO<sub>2</sub> gas (99.9 % purity)  
46 passed through a mass flow controller (GFC57 configured for CO<sub>2</sub>, Aalborg Instruments and Controls, Inc. Orangeburg, NY, USA)  
47 to a manifold (17 L) having outlets for each of the 10 pipes. Gas outlets of 1/16" (1.6 mm) diameter were placed every 50 cm along  
48 each pipe. We assumed equal flow rates from each outlet due to the high head loss across each outlet relative to the manifold  
49 pressure (following the argument made by Flesch et al., 2004).

50 The vertical CO<sub>2</sub> flux downwind of the synthetic source was measured using the eddy covariance (EC) technique. The  
51 instrumentation included a fast-response CO<sub>2</sub>/H<sub>2</sub>O analyser (Li-7500DS, Licor Biosciences, Lincoln, NE, USA) and a sonic  
52 anemometer (CSAT-3, Campbell Scientific, Logan, UT, USA) co-located at a height of 1.97 m above ground. The 10 Hz  
53 concentration and wind measurements were processed using the EddyPro® open source software (version 6.2.1 LI-COR  
54 Biosciences, Lincoln, NE, USA) to obtain 10 minute (min) average fluxes of CO<sub>2</sub>. The flux calculation applied a double coordinate  
55 wind rotation, Webb-Pearman-Leuning correction terms for density fluctuations (Webb et al., 1980), and spectral corrections for  
56 inadequate high and low frequency response of the sensors (Moncrieff et al., 1997, 2004). Quality checks for steady state conditions  
57 and integral turbulence characteristics were used to exclude error-prone periods (Foken and Wichura, 1996).

58 Gas releases took place over nine days, with the center of the synthetic source positioned (Fig. 1) at one of three nominal distances  
59 from the EC system (fetches of 15, 30, and 50 m). Placement of the source relative to the EC system depended on the expected  
60 wind direction. Because CO<sub>2</sub> is naturally emitted from the landscape it was important that the synthetic CO<sub>2</sub> release rate be  
61 sufficiently high so as to create a measured atmospheric flux that was many times larger than the natural landscape flux. Nicolini  
62 et al. (2017) found a CO<sub>2</sub> release rate of 22 L min<sup>-1</sup> was sufficient to distinguish the release signal from background levels. Our  
63 situation was helped in that the experiment took place during the dormant autumn season when landscape CO<sub>2</sub> fluxes were small.  
64 Gas was released at rates between 30 and 90 L min<sup>-1</sup>, with larger rates used for the larger fetches. Prior to any release interval, and  
65 immediately after each hour of gas release, a 30 min period of background CO<sub>2</sub> flux was measured. These background fluxes  
66 (which were consistently small) were subtracted from the EC measured fluxes prior to undertaking the footprint analyses.

67 Our study consisted of more than 300 10 min flux measurement periods, and included periods of gas release, background flux  
68 measurements, and transitions when gas was released but a steady state plume may not have been established over the field site  
69 (we assumed this occurred 10 min after gas was turned on). There was a total of 125 valid gas release periods. From this total we  
70 excluded 66 periods from our analysis based on two broad factors:

- 71 • 19 periods were excluded for having wind conditions associated with unreliability in the EC measurements or the  
72 dispersion model calculations: light winds with a friction velocity  $u^* < 0.05 \text{ m s}^{-1}$ , or an inferred roughness length  $z_0 >$   
73  $0.25 \text{ m}$ . A low  $u^*$  filtering criterion is often used in EC analyses (e.g., Rannik et al., 2004) and in dispersion model  
74 calculations (e.g., Flesch et al., 2014). The  $z_0$  filtering criterion indicates an unrealistic wind profile given the bare soil  
75 conditions of our site, and the likelihood of inaccurate dispersion model calculations given that wind profile.

76 • 47 periods were excluded when the EC measurement location was not obviously in the source plume. This included  
77 periods when the measured CO<sub>2</sub> flux was less than zero, when the wind direction deviated more than 30 degrees from the  
78 line between the EC site and the source center, or when the LS footprint model (described below) indicated the plume  
79 may not have reached the EC measurement site (i.e., fewer than 1,000 of 1,000,000 backward trajectories released from  
80 the EC site reached the source).

81 These quality control criteria eliminated over half of the gas release periods, leaving 59 periods for the footprint analysis. The  
82 final data are provided in the supplemental material accompanying this report.

## 83 **2.2 Flux Footprint Models**

### 84 **2.2.1 Kormann and Meixner (KM) Model**

85 The KM model is based on an analytical solution to the steady-state advection-diffusion equation, assuming simplified power-law  
86 profiles for windspeed and eddy diffusivity, and a crosswind diffusion component (Kormann and Meixner, 2001). We used the  
87 ART Footprint Tool software (Spirig et al., 2007; Neftel et al., 2008) based on the KM model to calculate the synthetic source  
88 emission rate ( $Q_{KM}$ , g C m<sup>-2</sup> s<sup>-1</sup>) from the measured EC flux. The calculation uses the spatial outline of the source polygon, the EC  
89 measurement height ( $z_{EC}$ ), the horizontal wind speed at height  $z_{EC}$ , the friction velocity ( $u^*$ ), the standard deviation of the lateral  
90 wind velocity ( $\sigma_v$ ), and the Obukhov length ( $L$ ). The wind variables were measured with a 3-D sonic anemometer (part of the EC  
91 system). In this study, the ratio of the KM-calculated synthetic emission rate to the actual release rate ( $Q_{KM}/Q$ ) is the metric for  
92 model testing. A perfectly accurate calculation gives  $Q_{KM}/Q = 1$ .

### 93 **2.2.2 Lagrangian Stochastic (LS) Model**

94 A state of the art LS model was also used to calculate the emission rate from the synthetic source ( $Q_{LS}$ , g C m<sup>-2</sup> s<sup>-1</sup>) based on the  
95 measured EC flux. The relationship between the source emission rate and the EC flux was calculated from the trajectories of  
96 thousands of model “particles” travelling upwind from the EC measurement point (backward in time). We follow the calculation  
97 procedure outlined in Flesch (1996) using the LS model detailed in Flesch et al. (2004). This model uses the wind velocity  
98 fluctuations in the three directional components ( $\sigma_u$ ,  $\sigma_v$ ,  $\sigma_w$ ), the friction velocity ( $u^*$ ), the Obukhov stability length ( $L$ ), the average  
99 wind direction, and the surface roughness length ( $z_0$ ). These properties were calculated from the 3-D sonic anemometer  
100 measurements. The LS calculations were made using 1,000,000 particles for each 10 min observation interval. A perfectly accurate  
101 LS model calculation gives  $Q_{LS}/Q = 1$ .

## 102 **2.3 Statistical Analysis**

103 The accuracies of the footprint calculations are evaluated from the ratio of the model calculated emission rate to the actual release  
104 rate:  $Q_{KM}/Q$  and  $Q_{LS}/Q$ . These ratio data are asymmetrically distributed, and a logarithmic transform of the ratios is used when  
105 making our statistical comparisons. Thus, the geometric means of the emission ratios is our measure of central tendency.  
106 Confidence intervals for the geometric mean are calculated using the log-transformed ratio data, and then converted back to ratio  
107 units (Limpert et al., 2001). The confidence intervals (CI) are asymmetrical, and we report the upper and lower limits of the  
108 intervals.

### 109 3 Results and Discussion

110 The synthetic emission rates calculated with both footprint models underestimate the actual emissions by roughly 30% on average.  
111 The overall means of the footprint calculations, expressed as the ratio of the model calculated emission rate to the actual emission  
112 rate, are  $Q_{KM} / Q = 0.67$  (95% CI: 0.50, 0.89) and  $Q_{LS} / Q = 0.77$  (CI: 0.60, 0.98). These means are statistically less than 1.0, but  
113 not different from each other (paired t-tests with  $P_s > 0.05$ ). The period-to-period variability in the  $Q / Q$  ratios is large, with  $Q_{KM}$   
114  $/ Q$  ranging between 0.04 and 2.20 and  $Q_{LS} / Q$  between 0.06 and 4.44. Some of the variability is likely due to the small size of the  
115 area source. The 10 x10 m source covers a small portion of the entire flux footprint. As opposed to larger source areas, the small  
116 area should amplify the differences between the models, and increase the relative uncertainty in the footprint calculations (i.e.,  
117 increasing the size of the source area means increasing the spatial integration of the footprint function in the calculations, which  
118 acts to increasingly constrain the  $Q / Q$  values closer to one).

119 When examining the footprint agreements as a function of fetch (Fig. 2), we find both models are accurate at the shorter fetch of  
120 15 m, as the means of  $Q_{KM} / Q$  and  $Q_{LS} / Q$  are not statistically different from 1. At the 15 m fetch the  $Q_{KM}$  calculation tends to  
121 slightly overestimate the actual emission rate with  $Q_{KM} / Q = 1.17$  (CI: 1.00, 1.36), while  $Q_{LS}$  tends to slightly underestimates it  
122 with  $Q_{LS} / Q = 0.84$  (CI: 0.68, 1.04). Based on the calculations of Wilson (2015) and Heidbach et al. (2017), we had hypothesized  
123 that there would be substantial differences between the two models at the shorter fetch, with the LS model being more accurate  
124 than KM due to a better representation of horizontal turbulent transport, which is particularly important for defining the footprint  
125 at short fetches. However, this is not the case in this study. At the intermediate fetch of 30 m, the KM model slightly overestimates  
126 the emission rate with  $Q_{KM} / Q = 1.21$  (CI: 0.86, 1.71), while the LS model substantially overestimates it with  $Q_{LS} / Q = 1.75$  (CI:  
127 1.39, 2.21). At the larger 50 m fetch, both models substantially underestimate the emission rate, with  $Q_{KM}$  underestimating  $Q$  by  
128 a factor of three and  $Q_{LS}$  underestimating by a factor of two (on average). The underestimate of  $Q_{KM} / Q$  at the larger fetch is  
129 similar to findings by Talleg et al. (2012) and Felber et al. (2015).

130 In Figure 3 we show the  $Q / Q$  ratios grouped according to atmospheric stability. The observations are separated into three groups  
131 having nearly equal numbers of observations: neutral ( $|L| > 60$  m), unstable ( $0 > L > -60$  m), and stable ( $60 > L > 0$  m). For the  
132 neutral and unstable groups, the mean  $Q / Q$  from both models does not statistically differ from 1, nor does it differ between groups  
133 due to the large variability in the calculations. However, in stable conditions both models are inaccurate and they substantially  
134 underestimate the actual emission rate. A more detailed look at the stable cases shows the  $Q_{KM} / Q$  calculations are particularly  
135 inaccurate for the 50 m fetch, with a mean of 0.14 (CI: 0.03, 0.62).

136 There are no clear patterns in terms of explaining the differences between the two footprint models based on environmental factors.  
137 Whether we separate the data by fetch or by stability, the results from the two models are not statistically different from each other.  
138 Wind speed, roughness length, and wind direction (deviation from a line between the EC system and the source) were also  
139 considered as factors to explain the model differences, but again, no pattern was observed. The lack of model differences was  
140 unexpected given the studies of Göckede et al. (2005), Wilson (2015), and Heidbach et al. (2017) showing large differences in the  
141 calculations between analytical and LS models. This suggests that in our study, any systematic differences between the models  
142 were obscured by the substantial period-to-period variability in the  $Q / Q$  calculations, and that the detection of model differences  
143 would require a much larger observational sample size than we were able to acquire.

144 **4 Conclusions**

145 From an end-user's perspective, our results show that both the KM and LS models returned reasonably accurate flux footprint  
146 estimates on average, particularly for the shorter measurement fetches. Our dataset does not consistently discriminate between the  
147 performance of the two models, despite the theoretical advantages of the LS model. Based on the results of this study, we conclude  
148 that the easy to use KM model can provide accurate footprint calculations that are accessible to non-specialists.

149 It is clear that the KM and LS footprint models give systematically different results (as shown in Wilson 2015); but that we were  
150 unable to (statistically) observe these differences given the large period-to-period variability in the calculations and the relatively  
151 small number of field observations. The small area of our synthetic source likely contributed to the large variability, and a larger  
152 source may have allowed better differentiation between the models. However, period-to-period variability is the nature of footprint  
153 calculations based on simplified models of atmospheric transport like the KM and LS formulations. These model calculations,  
154 which at best approximate an ensemble average realization of the atmosphere, will not reflect the period-to-period fluctuations of  
155 actual measurement periods.

156 **Data availability**

157 The data used in this analysis are available as supplementary material, or by request to Trevor.Coates@Canada.ca.

158 **Author contributions**

159 TC analyzed the field data and helped write the manuscript. MA design the experiment, and coordinated and collected the field  
160 data. TF helped with the experimental design and data analysis, and reviewed the manuscript. GHR helped with the experimental  
161 design and reviewed the manuscript.

162 **Competing interests**

163 The authors declare that they have no conflict of interest.

164 **Acknowledgements**

165 The authors gratefully acknowledge funding from Canada Foundation for Innovation – John Evans Leadership Fund, Natural  
166 Sciences and Engineering Research Council of Canada – Discovery Grant, and Agriculture and Agri-Food Canada – Agricultural  
167 Greenhouse Gases Program 2, as well as assistance from Dick Puurveen and Sheilah Nolan.

168 **References**

169 Budishchev, A., Mi, Y., van Huissteden, J., Belelli-Marchesini, L., Schaepman-Strub, G., Parmentier, F.J.W., Fratini, G.,  
170 Gallagher, A., Maximov, T.C., and Dolman, A.J.: Evaluation of a plot-scale methane emission model using eddy covariance  
171 observations and footprint modelling, *Biogeosci.*, 11, 4651–4664, <https://doi.org/10.5194/bg-11-4651-2014>, 2014.  
172 Coates, T.W., T.K. Flesch, S.M. McGinn, E. Charmley, and D. Chen. 2017. Evaluating an eddy covariance technique to estimate  
173 point-source emissions and its potential application to grazing cattle. *Agric. Forest. Meteorol.* 234-235:164-171.

174 Dyer, A.J.: The adjustment of profiles and eddy fluxes, *Q. J. R. Meteorol. Soc.*, 8:30, 276-280,  
175 <https://doi.org/10.1002/qj.49708938009>, 1963.

176 Felber, R., Munger, A., Neftel, A., and Ammann, C.: Eddy covariance methane flux measurements over a grazed pasture: Effect  
177 of cows as moving point sources, *Biogeosci.*, 12, 3925-3940, <https://doi.org/10.5194/bg-12-3925-2015>, 2015.

178 Flesch, T.K.: The footprint for flux measurements, from backward Lagrangian stochastic models, *Boundary-Layer Meteorol.*, 78,  
179 399-404, <https://doi.org/10.1007/BF00120943>, 1996.

180 Flesch, T.K., McGinn, S.M., Chen, D., Wilson, J.D., and Desjardins, R.L.: Data filtering for inverse dispersion calculations. *Agric.*  
181 *For. Meteorol.* 198-199, 1-6, <https://doi.org/10.1016/j.agrformet.2014.07.010>, 2014.

182 Flesch, T.K., Wilson, J.D., Harper, L.A., Crenna, B.P., and Sharpe, R.R.: Deducing ground-to-air emissions from observed trace  
183 gas concentrations: A field trial, *J. Appl. Meteorol. and Climatol.*, 43, 487-502, [https://doi.org/10.1175/1520-0450\(2004\)043<0487:DGEFOT>2.0.CO;2](https://doi.org/10.1175/1520-0450(2004)043<0487:DGEFOT>2.0.CO;2), 2004.

185 Foken, T., and Wichura, B.: Tools for quality assessment of surface-based flux measurements, *Agric. For. Meteorol.*, 78, 83-105,  
186 doi: 10.1016/0168-1923(95)02248-1, 1996.

187 Gockede, M., Markkanen, T., Mauder, M., Arnold, K., Leps, J. P., and Foken, T.: Validation of footprint models using natural  
188 tracer measurements from a field experiment, *Agric. For. Meteorol.*, 135, 314-325,  
189 <https://doi.org/10.1016/j.agrformet.2005.12.008>, 2005.

190 Heidbach, K., Schmid, H.P., and Mauder, M.: Experimental evaluation of flux footprint models. *Agric. For. Meteorol.*, 247, 142-  
191 153, <https://doi.org/10.1016/j.agrformet.2017.06.008>, 2017.

192 Kljun, N., Rotach, M.W., and Schmid, H.P.: A three-dimensional backward Lagrangian footprint model for a wide range of  
193 boundary-layer stratifications, *Boundary-Layer Meteorol.*, 103, 205–226, <https://dx.doi.org/10.1023/A:1014556300021>, 2002.

194 Kormann, R., and Meixner, F.X.: An analytical footprint model for non-neutral stratification, *Boundary-Layer Meteorol.*,  
195 <https://doi.org/10.1023/A:1018991015119>, 2001.

196 Limpert, E., Stahel, W.A., and Abbt, M.: Log-normal distributions across the sciences: keys and clues. *BioSci.* 51, 341-352, 2001.

197 Moncrieff, J., Clement, R., Finnigan, J., and Meyers, T.: Averaging, detrending, and filtering of eddy covariance time series, in:  
198 *Handbook of Micrometeorology: A Guide for Surface Flux Measurement and Analysis*, <https://doi.org/10.1007/1-4020-2265-4>,  
199 2004.

200 Moncrieff, J.B., Massheder, J.M., de Bruin, H., Elbers, J., Friborg, T., Heusinkveld, B., Kabat, P., Scott, S., Soegaard, H., and  
201 Verhoef, A.: A system to measure surface fluxes of momentum, sensible heat, water vapour and carbon dioxide, *J. Hydrol.*, 188-  
202 189, 589-611, [https://doi.org/10.1016/S0022-1694\(96\)03194-0](https://doi.org/10.1016/S0022-1694(96)03194-0), 1997.

203 Neftel, A., Spirig, C., and Ammann, C.: Application and test of a simple tool for operational footprint evaluations, *Environ. Pollut.*,  
204 152, 644-652, <https://doi.org/10.1016/j.envpol.2007.06.062>, 2008.

205 Nicolini, G., Fratini, G., Avilov, V., Kurbatova, J.A., Vasenev, I., and Valentini, R.: Performance of eddy-covariance  
206 measurements in fetch-limited applications, *Theoret. Appl. Climatol.*, 127, 829–840., <https://doi.org/10.1007/s00704-015-1673-x>,  
207 2017.

208 Rannik, Ü., Keronen, P., Hari, P., and Vesala, T.: Estimation of forest-atmosphere CO<sub>2</sub> exchange by eddy covariance and profile  
 209 techniques. *Agric. For. Meteorol.* 126, 141-155, <https://doi.org/10.1016/j.agrformet.2004.06.010>, 2004.

210 Schmid, H.P.: Footprint modeling for vegetation atmosphere exchange studies: A review and perspective, *Agric. For. Meteorol.*,  
 211 113, 159-183, [https://doi.org/10.1016/S0168-1923\(02\)00107-7](https://doi.org/10.1016/S0168-1923(02)00107-7), 2002.

212 Sogachev, A., and Lloyd, J.: Using a one-and-a-half order closure model of the atmospheric boundary layer for surface flux  
 213 footprint estimation, *Boundary-Layer Meteorol.*, 112, 467–502, <https://dx.doi.org/10.1023/B:BOUN.0000030664.52282.ee>, 2004.

214 Spirig, C., Flechard, C.R., Ammann, C., and Neftel, A.: The annual ammonia budget of fertilised cut grassland - Part 1:  
 215 Micrometeorological flux measurements and emissions after slurry application, *Biogeosci.*, 7, 521-536,  
 216 <https://doi.org/10.5194/bg-7-521-2010>, 2010.

217 Spirig, C., Ammann, C., and Neftel, A.: The ART Footprint Tool. (Version 1.0, 13 March 2007),  
 218 <https://zenodo.org/record/816236#.YVJoIn1MFhF>, 2007.

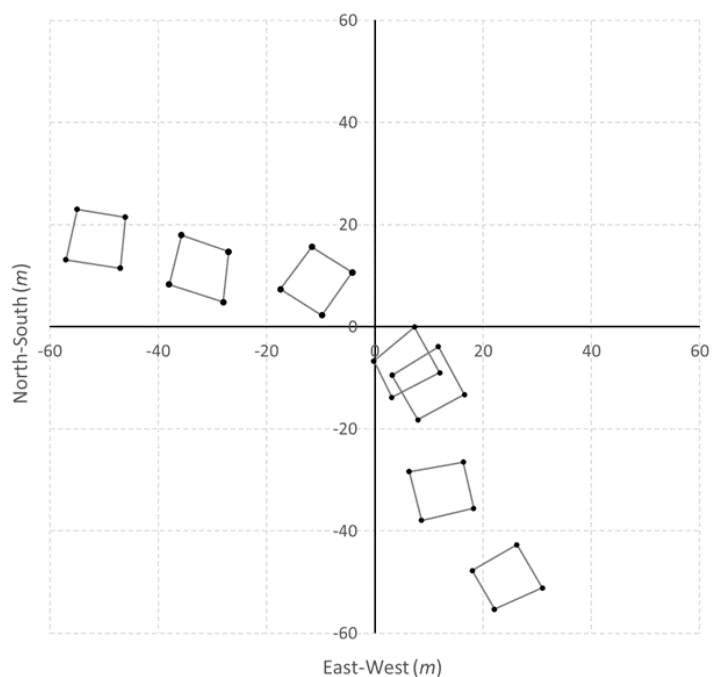
219 Stevens, R.M., Ewenz, C.M., Grigson, G., and Conner, S.M.: Water use by an irrigated almond orchard, *Irrig. Sci.*, 30, 189-200,  
 220 [doi.org/10.1007/s00271-011-0270-8](https://doi.org/10.1007/s00271-011-0270-8), 2012.

221 Tallec, T., Klumpp, K., Hensen, A., Rochette, Y., and Soussana, J.-F.: Methane emission measurements in a cattle grazed pasture:  
 222 a comparison of four methods, *Biogeosci. Discuss.*, 9, 14407-14436, <https://doi.org/10.5194/bgd-9-14407-2012>, 2012.

223 Webb, E.K., Pearman, G.I., and Leuning, R.: Correction of flux measurements for density effects due to heat and water vapour  
 224 transfer, *Q. J. R. Meteorol. Soc.*, 106, 85-100, <https://doi.org/10.1002/qj.49710644707>, 1980.

225 Wilson, J.D.: Computing the Flux Footprint, *Boundary-Layer Meteorol.*, 156, 1-14, <https://doi.org/10.1007/s10546-015-0017-9>,  
 226 2015.

227  
 228

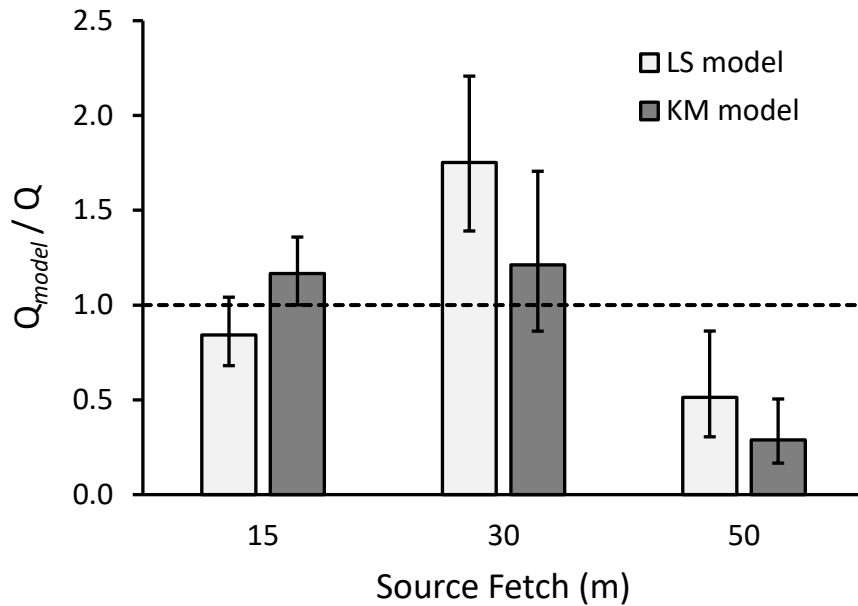


229

230 **Figure 1: Map of the synthetic source locations used in the study (polygons). The eddy covariance system was located at position (0,0).**

231

232

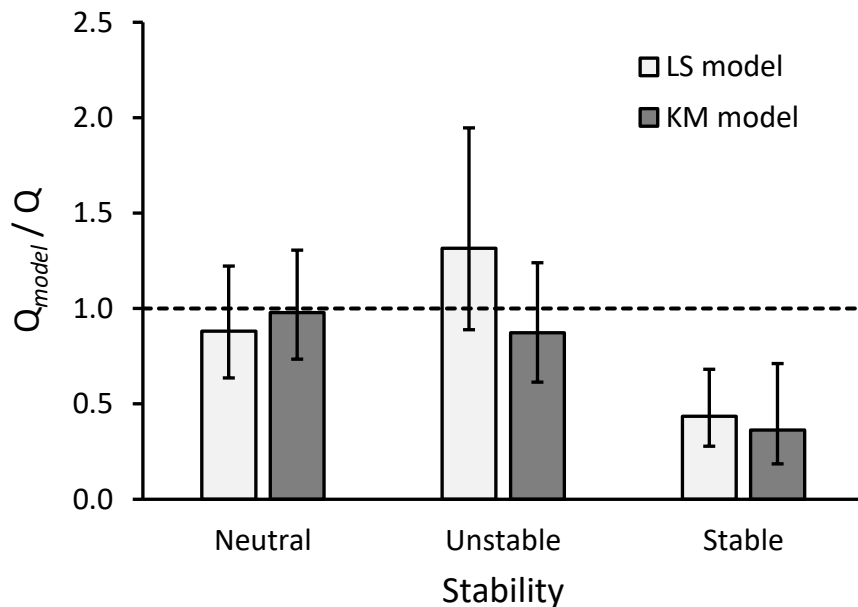


233

234 **Figure 2: Agreement ratio of the footprint model calculated emission rate ( $Q_{\text{model}}$ ) to actual release rate ( $Q$ ), grouped by source fetch of**  
235 **15 m (n = 26), 30 m (n = 9), and 50 m (n = 24). Calculations are from the LS and KM models. The columns show the geometric mean,**  
236 **and the error bars show the 95% confidence interval of the mean. The horizontal dashed line represents a  $Q_{\text{model}} / Q$  ratio of one, or a**  
237 **perfect model calculation.**

238

239



240

241 **Figure 3: Agreement ratio of the footprint model calculated emission rate ( $Q_{\text{model}}$ ) to actual release rate ( $Q$ ), grouped by atmospheric**  
242 **stability: neutral ( $|L| > 60$  m), unstable ( $0 > L > -60$ ), and stable ( $60 > L > 0$ ). Calculations are from the LS and KM models. The columns**  
243 **show the geometric mean, and the error bars show the 95% confidence interval of the mean. The horizontal dashed line represents a**  
244  **$Q_{\text{model}} / Q$  ratio of one, or a perfect model calculation.**